Desalination and Water Treatment
www.deswater.com

doi: 10.5004/dwt.2021.27284

227 (2021) 404–411
July

Kahwa tea (*Camellia sinensis*) carbon — a novel and green low-cost adsorbent for the sequestration of Titan yellow dye from its aqueous solutions

Jyoti Mittal[a], Rais Ahmad[b], Alok Mittal[c,*]

[a]*Department of Chemistry, Maulana Azad, National Institute of Technology, Bhopal 462003, India, email: jyalmittal@yahoo.co.in*
[b]*Environmental Research Laboratory, Department of Applied Chemistry, Aligarh Muslim University, Aligarh 202002, India, email: rais45@rediffmail.com*
[c]*Department of Chemistry, Maulana Azad, National Institute of Technology, Bhopal 462003, India, Tel. +91-9425025427; email: aljymittal@gmail.com*

Received 17 February 2021; Accepted 1 April 2021

ABSTRACT

The present study aims to explore the adsorption behavior of novel Kahwa tea (*Camellia sinensis*) carbon (KTC) towards its potential application as an adsorbent for the sequestration of Titan yellow (TY) dye from an aqueous solution. The maximum adsorption of TY from aqueous solution was observed at pH 5, contact time 180 min, initial concentration of dye 100 mg L^{-1} and temperature 318 K. The adsorption process follows a pseudo-second-order rate kinetic model and is in good agreement with the kinetic data. The equilibrium adsorption data fitted well with the Langmuir isotherm model with a maximum monolayer adsorption capacity of 55.55 mg g^{-1}, at 318 K. The thermodynamic parameters confirm the endothermic and spontaneous nature of the adsorption process with increased randomness. The desorption study predicts the excellent regenerative power of KTC.

Keywords: Camellia sinensis; Kahwa tea carbon; Adsorption; Titan yellow; Kinetics; Regeneration

1. Introduction

Azo dyes are a class of colored organic compounds, which are extensively used in textile, paper, leather, etc. industries [1]. During dye production and coloring of textile materials, a large quantity of wastewaters containing intensive color dyestuffs are accidentally introduced into the aquatic systems [2]. The toxicity of azo dyes towards humans, birds and animals is well known and all the derivatives of the azo class pose severe health damage to the extent of mutagenicity and carcinogenicity [3,4]. Moreover, the color intensity of azo dyes is so much fast and intense that the presence of even less than 1 ppm of dye is clearly visible and considerably influences the water environment [1,2,5]. Hence, removal of these colors from wastewater is a necessity and various methods have been adopted to eradicate azo dyes from wastewaters.

In the past three decades, physicochemical and biological methods such as adsorption, precipitation, photocatalytic degradation, flotation, ion exchange, oxidation, bacterial and fungal biosorption and biodegradation (aerobic and anaerobic) have been employed to remove azo dyes from wastewaters [6–10]. Amongst multiple approaches employed so far for the removal of dyestuffs and other pollutants, adsorption has attracted much attention due to advantages such as high efficiency, ease of use, low energy consumption, and cost-effectiveness [11–18]. Nevertheless, some shortcomings have been reported for previous routine adsorbents, including unacceptable reusability, weak

* Corresponding author.

adsorption capacity, and slow adsorption rate, highlighting the need for new adsorbents capable of overcoming such weak points [19]. In recent times, intense researches are going on to search for eco-friendly, waste material adsorbents for wastewater treatment. A green low-cost adsorbent not only helps in sustaining the environment but also reduces the cost of the treatment. The availability of the waste materials in abundance has further led to harness many such materials reported elsewhere [20–22].

The present paper is an attempt to eradicate the azo dye, 'Titan yellow' (TY) using Kahwa tea (*Camellia sinensis*) carbon (KTC). The dye TY is soluble in water and available as a slightly brown powder. It is widely used for dyeing a variety of textile materials like wool and nylon. The dye possesses potent toxicity and causes severe irritations in the eyes, skin, digestive tract, and respiratory tract [3,4]. Keeping the toxicity of dye in view, it was considered worthwhile to develop a systematic research module to eradicate it from the wastewater through adsorption over waste material, the used Kahwa tea. In the present paper, KTC is obtained after pyrolysis of Kahwa tea and used as a potential adsorbent for the removal of TY. Literature survey reveals that so far KTC has never been employed as an adsorbent for the removal of dyes, therefore it is a novel and green potential adsorbent for the sequestration of TY dye from wastewater.

Thus the present study focuses on the preparation of novel and eco-friendly KTC which has a very high adsorption capacity for the eradication of TY dye from its aqueous solutions. Paper is devoted to examining the effect of pH, contact time, initial dye concentration and temperature on the adsorption of the dye onto KTC. The experimental adsorption data have been applied to Langmuir and Freundlich isotherm models. The kinetic studies have been carried out by using pseudo-first and pseudo-second-order models. To enhance the scope of the laboratory-developed process to an industrial scale, attempts have also been made to remove the bulk amount of dye through adsorption and later dye recovery and regeneration of adsorbent was by adopting desorption procedures.

2. Materials and methods

2.1. Materials and reagents

Kahwa tea (KT) was procured from the local market. Analytical grade hydrochloric acid (HCl) and sodium hydroxide (NaOH) were used. The disodium salt of TY, molecular formula $C_{28}H_{19}N_5Na_2O_6S_4$, molecular mass 695.72 g mol^{-1} and λ_{max} 402 nm was procured from M/s Merck, India. The stock solution of dye (1,000 mg L^{-1}) was prepared by dissolving the required amount of dye in double-distilled water.

2.2. Preparation of KTC

The procured KT was first washed with double distilled water to remove the adhering dirt and then dried in the oven at 80°C. The dried materials were then placed in the muffle furnace for 1 h maintained at 750°C. The resultant carbon thus obtained KTC was grounded, sieved (50–100 mesh size), washed with double distilled water, dried out and stored in a desiccator till further use. The specific surface area of the KTC has been evaluated as 44.12 m^2 g^{-1}.

2.3. Characterization

The elemental analysis and surface morphology of the KTC before and after adsorption were examined by scanning electron microscopy (SEM) equipped with an energy-dispersive X-ray spectrometer (EDX, Model JSM-6510LV, JEOL, Japan). The particle size of KTC was examined by high-resolution transmission electron microscope Tecnai G^2 20 (M/s TSS Microscopy, USA). Fourier-transform infrared spectroscopy (FTIR) measurements were recorded in the range of 400–4,000 cm^{-1} with a Nicolet iS50 FTIR spectrometer (M/s Thermo Fisher, USA) by preparing sample pellets in KBr. X-ray diffraction (XRD) pattern was carried out using Bruker (USA) AXS D8 Advance X-ray diffractometer Bruker (M/s Bruker Corporation, USA) with Cu α radiation (λ = 1.542 Å).

2.4. Batch adsorption experiments

For batch adsorption experiments, 20 mL of TY of known initial concentration along with 0.01 g of KTC were taken in a series of conical flasks at constant pH and temperature and mixtures were thoroughly shaken for a fixed interval of contact time. The studies were conducted by varying the initial dye concentration, pH, contact time, KTC dosage and temperature. The initial pH values of the samples were adjusted using dilute HCl and dilute NaOH solutions. After treatment of dye solutions with KTC, the samples were filtered using Whatman No 1 filter paper and the concentration of filtrate samples was then determined using UV-Vis spectrophotometer (T70 UV/VIS Spectrometer, M/s PG Instruments Ltd., UK) at 402 nm the λ_{max} of TY. The λ_{max} 402 was measured experimentally and matched with the available literature [23]. The amount of dye adsorbed per unit mass of the adsorbent q_e (mg g^{-1}) and the extent of adsorption (%) was calculated using the following equations:

$$q_e = \frac{C_i - C_e}{m} \times V \tag{1}$$

$$\% = \frac{C_i - C_e}{C_i} \times 100 \tag{2}$$

where C_i and C_e are the initial and final dye concentration after adsorption (mg L^{-1}), m is the mass of the adsorbent (g) and V is the initial volume of the dye Eq. (l), respectively [24].

2.5. Error analysis

In the non-linear-regression, R^2, normalized standard deviation (Δq) and χ^2 were employed as the judging criteria to compare the experimental and model-predicted data. The equivalent mathematical equations reported elsewhere [25] are as follows:

$$\chi^2 = \sum_{i=1}^{n} \frac{\left(q_{e,\text{cal}} - q_{\text{exp}}\right)^2}{q_{e,\text{exp}}} \tag{3}$$

$$R^2 = \frac{\sum\left(q_{e,\text{exp}} - \bar{q}_{e,\text{cal}}\right)^2}{\sum\left(\left(q_{e,\text{exp}} - \bar{q}_{e,\text{cal}}\right)^2 + \left(q_{e,\text{exp}} - q_{e,\text{cal}}\right)^2\right)} \tag{4}$$

$$\Delta q = \sqrt{\frac{\sum\left(\frac{q_{e,\exp} - q_{e,\text{cal}}}{q_{e,\exp}}\right)^2}{n-1}} \quad (5)$$

where n represents the number of performed runs, $q_{e,\text{cal}}$ is the equilibrium capacity obtained by calculation from the fitted model (mg g^{-1}). Also, $q_{e,\text{cal}}$ is the average of the calculated uptake and $q_{e,\exp}$ is the equilibrium capacity (mg g^{-1}) from the experimental data. Smaller amounts of Δq and values of χ^2 and R^2 closer to unity provide better fitting results.

2.5. Desorption and regeneration studies

KTC particles exhausted by the adsorption of the dye TY were regenerated and recovery of dye was made using 0.1 M HCl. The regenerated KTC was reused for the next set of adsorption and in this way, several adsorption/desorption cycles were performed. With the help of adsorbed and desorbed dye amounts, the percentage saturation of the KTC were evaluated.

3. Results and discussion

3.1. Characterization

3.1.1. SEM and EDX analysis

The SEM images of before and after adsorption of TY dye molecules onto the surface of the KTC particle are shown in Figs. 1a and b. The SEM image presented in Fig. 1a exhibits the highly cross-linked and porous structure of KTC, which provides sufficient sites for the adsorption of TY molecules. The cloudy surface appearance of the SEM image (Fig. 1b) confirms the successful adsorption of dye molecules onto the surface of KTC.

The EDX and elemental analysis of KTC before and after treatment of TY dye are shown in Fig. 2 and Table 1, respectively. The EDX of KTC shows the presence of C, O and K, while the dye adsorbed KTC exhibits the presence of C, O, K, Na and S elements. The presence of Na and S in the TY dye adsorbed KTC spectrum further confirms the adsorption of TY dye onto the surface of KTC.

3.1.2. FTIR analysis

FTIR spectra of KTC and TY adsorbed KTC are represented in Fig. 3. The FTIR spectra showed strong broad peak at 3,436 cm^{-1} (O–H stretching), 2,929 cm^{-1} (C–H stretching), 1,737 cm^{-1} (asymmetric –COO stretching), 1,625 cm^{-1} (symmetric –COO stretching), 1,025 cm^{-1} (stretching vibration of C–OH group), 609 cm^{-1} and 433 cm^{-1} (C–C–O, C–C–H bending), respectively. Whereas, the TY loaded adsorbent showed peaks at 3,430; 2,923; 1,752; 1,632; 1,019; 644 and 448 cm^{-1}, respectively have been also reported elsewhere [26,27]. There is shifting of peaks in KTC after being treated with TY dye, indicating thereby successful adsorption of the dye onto the surface of KTC.

3.2. Effect of pH on adsorption

The pH of the dye solution greatly affects the adsorption process by influencing the surface charge of the adsorbent and also the degree of ionization of adsorbate dye species. The tests for the effect of pH (ranging 2–9) on the adsorption process were carried out at experimental conditions taking dye concentration 20 mg L^{-1}, adsorbent dose 0.01 g, contact time 240 min, and temperature 298 K. It can be observed from Fig. 4 that the adsorption capacity (q_e) first increases with increase in pH and reaches to a maximum at pH 5.0. After pH 5.0, there is a sharp decrease in adsorption capacity till pH 9.0. This can be attributed to the fact that with the increase in pH of the medium, the charge on the surface of the adsorbent changes due to deprotonation and an electric double layer is formed around the adsorbent, which changes the polarity of the dye molecule and consequently the dye uptake increases. After maxima are attained, further increase in pH results in a decrease in protonation and electrostatic repulsive force becomes operative, which thereby retards diffusion and adsorption. Similar results are also reported elsewhere [28,29]. All further experimental studies were carried out at pH 5.0.

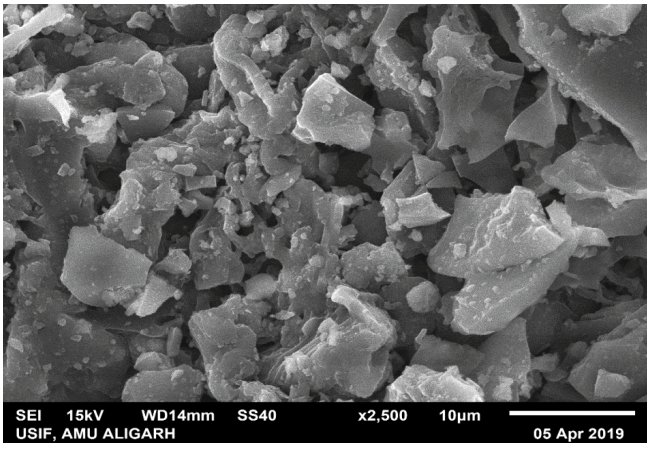

(a)

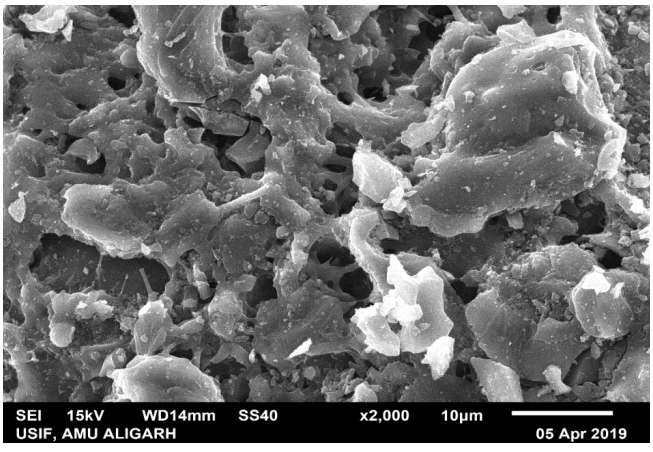

(b)

Fig. 1. SEM micrograph (a) before and (b) after adsorption of Titan yellow dye on Kahwa tea carbon.

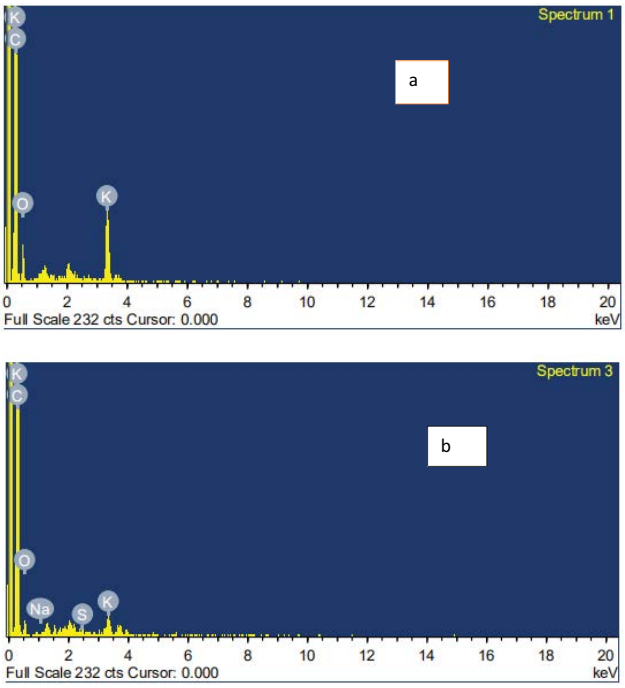

Fig. 2. EDX micrograph (a) before and (b) after adsorption of Titan yellow dye on Kahwa tea carbon.

Table 1
Elemental analysis of Kahwa tea carbon before and after adsorption of Titan yellow dye

Elements	% Before adsorption	% After adsorption
C	78.90	89.66
O	18.97	9.64
Na	Nil	0.08
S	Nil	0.01
K	2.13	0.60

3.3. *Effect of contact time and adsorption kinetics*

The test for the effect of contact time (ranging 5 to 750 min) on the adsorption process was monitored by taking dye concentration 20 mg L^{-1}, adsorbent dosage 0.01 g, pH 5 and temperature 298 K. Fig. 5 exhibits that the adsorption of the dye increases with increasing contact time and equilibrium is attained after 180 min. The increase in adsorption of the dye in the initial stages is due to the high availability of adsorption sites over adsorbents. At equilibrium, all the vacant sites have been occupied by the dye molecules and a plateau is reached beyond 180 min of contact time. Therefore, for all further experimental studies contact time of 180 min was selected.

The rate of the adsorption process was investigated using pseudo-first and pseudo-second-order kinetic models, as expressed by following mathematical expressions Eqs. (6) and (7), respectively:

$$\log\left(q_e - q_t\right) = \log q_e - \frac{k_1 t}{2.303} \tag{6}$$

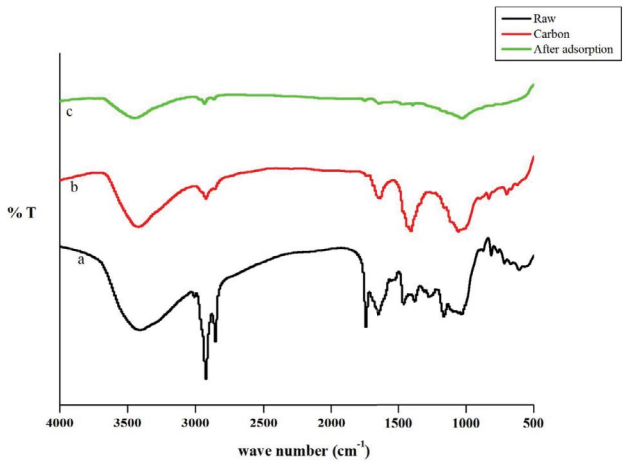

Fig. 3. FTIR analysis before and after adsorption of Titan yellow dye on Kahwa tea carbon.

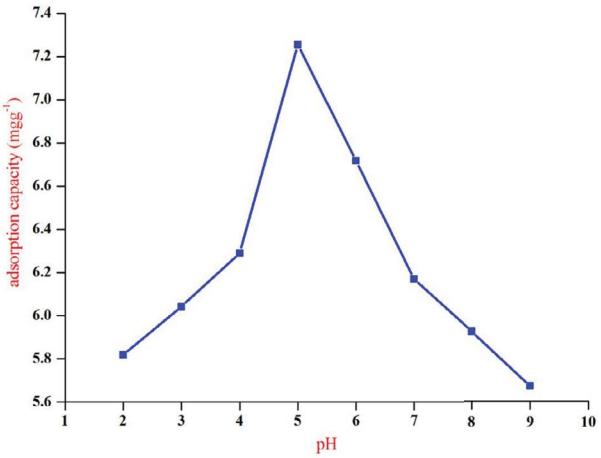

Fig. 4. Effect of pH on the adsorption of Titan yellow dye on Kahwa tea carbon.

$$\frac{t}{q_t} = \frac{t}{q_e} + \frac{q_e^2}{k_2} \tag{7}$$

where q_e and q_t (mg g^{-1}) are the adsorption capacity at equilibrium and time t, k_1 (min^{-1}) and k_2 (g mg^{-1} min^{-1}) are the pseudo-first and pseudo-second-order rate constants, respectively. The graph for pseudo-first-order was plotted between $\log(q_e - q_t)$ vs. t (Fig. 6) and for pseudo-second-order rate expression between t/q_t vs. t (Fig. 7).

Figs. 6 and 7 clearly indicate that for both the model's straight lines are obtained, however, the value of correlation coefficient (R^2) obtained for the pseudo-second-order model is close to unity and higher as compared to the pseudo-first-order model. Thus the adsorption of TY over KTC is considered to follow pseudo-second-order kinetics. Several other dyes – adsorbent adsorption systems also follow a similar trend [30]. Values of rate constants, experimental q_e, calculated q_e, R^2 for both the models are presented in Table 2.

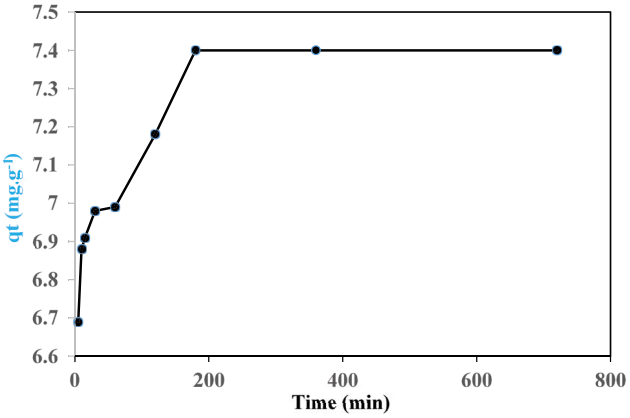

Fig. 5. Effect of contact time on the adsorption of Titan yellow dye on Kahwa tea carbon.

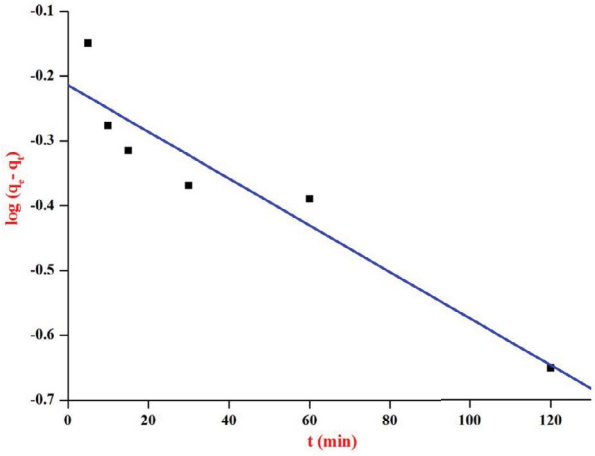

Fig. 6. Verification of pseudo-first-order kinetics on the adsorption of Titan yellow dye on Kahwa tea carbon.

3.4. Effect of initial dye concentration and adsorption isotherms

Effect of initial dye concentration (ranging from 20 to 100 mg L^{-1}) on adsorption process was carried out at experimental conditions taking adsorbent dose 0.01 g, pH 5, contact time 180 min and temperature 298 K (Fig. 8). As observed from Fig. 8, the adsorption capacity increases with increasing initial concentration at all temperatures that might be due to the increased concentration gradient between the bulk solution and the adsorbent surface also reported elsewhere [31].

The equilibrium data for the adsorption of TY over KTC was plotted (Fig. 9) and verified using Langmuir and Freundlich adsorption isotherm models, as expressed by Eqs. (8) and (9), respectively.

$$\frac{1}{q_e} = \frac{1}{C_e \cdot bq_m} + \frac{1}{q_m} \tag{8}$$

$$\log q_e = \log K_F + \frac{1}{n}\log C_e \tag{9}$$

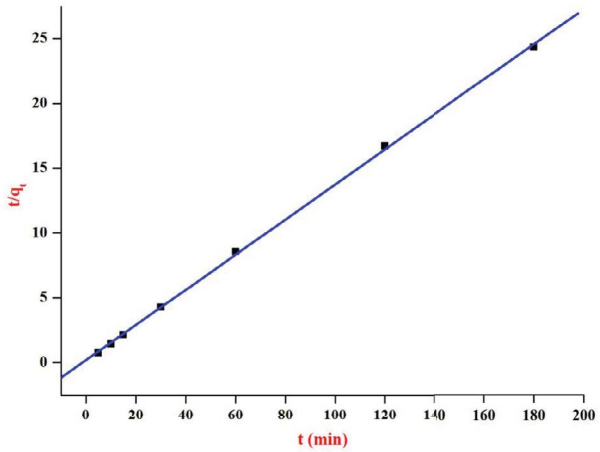

Fig. 7. Verification of pseudo-second-order kinetics on the adsorption of Titan yellow dye on Kahwa tea carbon.

where C_e and q_e are the equilibrium concentration (mg L^{-1}) and adsorption capacity at equilibrium (mg g^{-1}), b signifies the energy of adsorption (L mg g^{-1}), K_F (mg g^{-1})(L $mg^{-1})^{1/n}$ and n is the Freundlich constant related to adsorption capacity and adsorption intensity [32–34].

The Langmuir and Freundlich adsorption isotherm graphs are shown in Figs. 10 and 11, respectively. Based on the high correlation coefficient value (R^2), the Langmuir isotherm model was found to be the best-fitted isotherm with the equilibrium adsorption data (Table 3). The error functions (Δq and χ^2) of the experimental adsorption capacity were also calculated and found minimum in the case of the Langmuir isotherm model (Table 3).

3.5. Thermodynamics parameters of adsorption

Thermodynamic parameters like free energy change ($\Delta G°$), enthalpy change ($\Delta H°$) and entropy change ($\Delta S°$) for the adsorption of TY onto KTC were calculated from the following equations:

$$K_c = \frac{\left(C_i - C_e\right)}{C_e} \tag{10}$$

$$\Delta G° = -RT\ln K_c \tag{11}$$

$$\log K_c = \frac{\Delta S°}{2.303R} - \frac{\Delta H°}{2.303RT} \tag{12}$$

where T is the temperature (K), K_c is the distribution coefficient, C_i is the initial concentration (mg L^{-1}), C_e is the equilibrium concentration (mg L^{-1}) and R (JK^{-1} mol^{-1}) is the universal gas constant. The thermodynamic parameters $\Delta H°$ and $\Delta S°$ were evaluated from the plot of $\ln K_c$ vs. $1/T$ and presented in Fig. 12.

The thermodynamic parameters are tabulated in Table 4. The positive value of $\Delta H°$ and $\Delta S°$ for TY demonstrates that the adsorption onto the KTC is endothermic with increased randomness at solid/liquid interface during

Table 2
Kinetic parameters of the adsorption of Titan yellow dye on Kahwa tea carbon

Parameter	Value
Pseudo-first-order model	
k_1 (min^{-1})	0.0092
$q_{e,exp}$ (mg g^{-1})	7.400
$q_{e,cal}$ (mg g^{-1})	0.611
R^2	0.902
χ^2	6.228
Δq	0.094
Pseudo-second-order model	
k_2 (g mg^{-1} min^{-1})	0.0893
$q_{e,exp}$ (mg g^{-1})	7.400
$q_{e,cal}$ (mg g^{-1})	7.407
R^2	0.995
χ^2	0.987
Δq	1.001

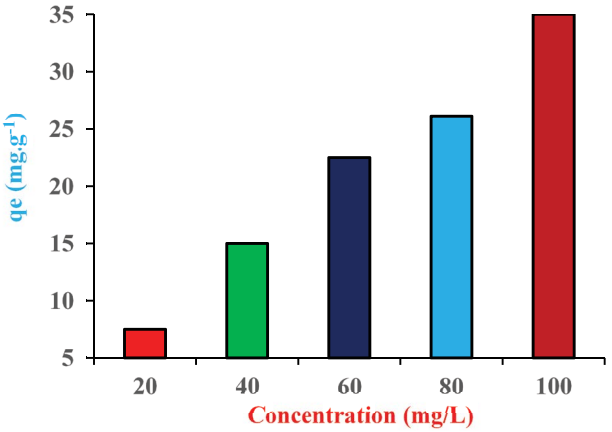

Fig. 8. Effect of concentration on the adsorption of Titan yellow dye on Kahwa tea carbon.

adsorption [35]. The negative value of $\Delta G°$ at all temperatures for TY showed the spontaneous nature of the ongoing adsorption [36].

3.6. Desorption and regeneration of adsorbent

As discarding of dye-loaded adsorbent in landfills creates pollution. So, it is always desirable to remove the dye from the adsorbent after adsorption using the desorption process. This also provides an opportunity to recover the costly dye material and reuse the adsorbent material. To carry out the desorption process the dye exhausted adsorbent was shaken with 0.1 M HCl solution. The results showed that in the first cycle 82% of TY dye was desorbed from the dye-loaded adsorbent. The process was repeated and good regeneration lasts up to the third cycles (65% desorption) without significant loss in adsorption capacity as shown in Fig. 13. Therefore, KTC has been proved to

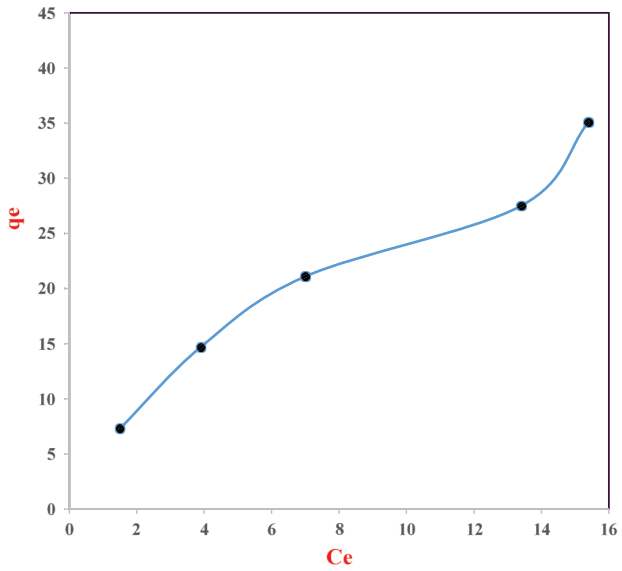

Fig. 9. Adsorption isotherm graph for the Titan yellow dye and Kahwa tea carbon system.

Table 3
Isotherm parameters of the adsorption of Titan yellow dye on Kahwa tea carbon at 30°C

Parameter	Value
Langmuir isotherm	
q_m (mg g^{-1})	55.55
b (L mg^{-1})	0.098
R^2	0.994
χ^2	1.040
Δq	0.094
Freundlich isotherm	
K_F (mg g^{-1})(L mg^{-1})$^{1/n}$	5.420
n	1.385
R^2	0.992
χ^2	8.84
Δq	0.145

be an excellent adsorbent with good regenerative capacity for the sequestration of TY dye from an aqueous solution.

4. Conclusions

The undertaken studies clearly indicate that the novel and eco-friendly adsorbent KTC can be very effectively employed for the removal of TY dye from its aqueous solutions. The material has been characterized using several techniques such as SEM, EDX, XRD and FTIR. The SEM results show that the material is porous and the involvement of functional groups in the adsorption of TY dye can be observed from FTIR spectra. The adsorption process is highly influenced by various factors such as contact time, initial concentration, dose, temperature and pH. On basis

Table 4
Thermodynamic parameters for the adsorption of Titan yellow dye on Kahwa tea carbon

Temperature (K)	$-\Delta G°$ (kJ mol^{-1})	$\Delta H°$ (kJ mol^{-1})	$\Delta S°$ (kJ K^{-1} mol^{-1})
303	6.331		
313	6.823	22.880	0.095
323	8.225		

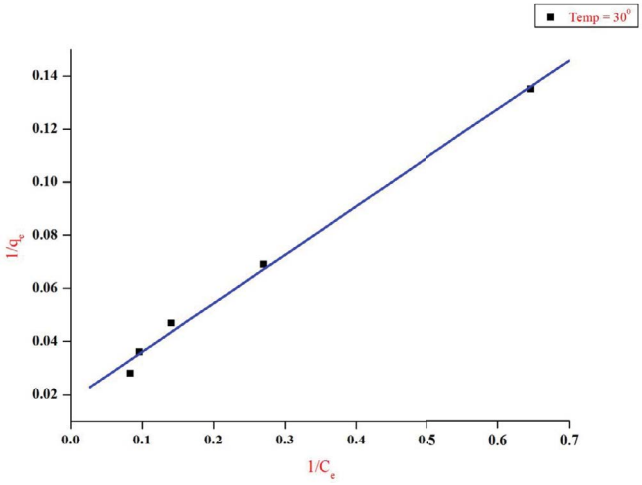

Fig. 10. Verification of Langmuir adsorption isotherm model for the Titan yellow dye and Kahwa tea carbon system.

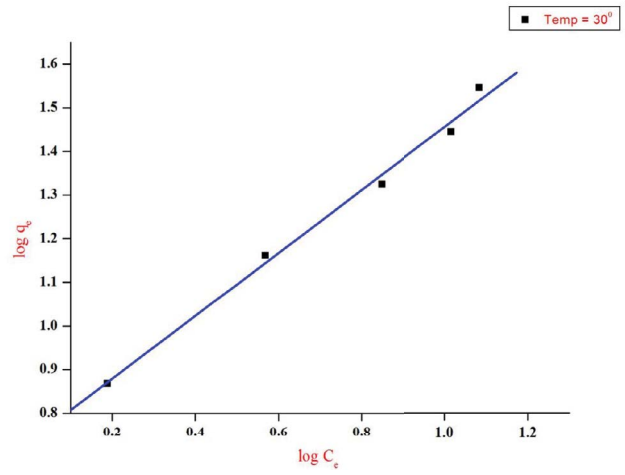

Fig. 11. Verification of Freundlich adsorption isotherm model for the Titan yellow dye and Kahwa tea carbon system.

of best-fitted plots, results clearly exhibit that ongoing adsorption follows Langmuir adsorption isotherm and pseudo-second-order models. The thermodynamic parameters further reveal the adsorption endothermic, spontaneous with increased randomness between solid/solution interface. During desorption, in the first cycle, 82% of the adsorbed dye could be desorbed by using 0.1 N HCl solution. Regeneration studies showed that adsorbent can be used successfully up to three cycles (65%) without significant loss in the adsorption capacity of the KTC.

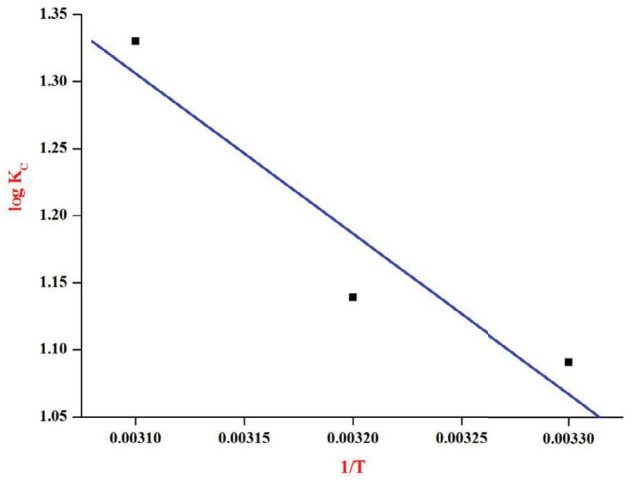

Fig. 12. Thermodynamic studies on the adsorption of Titan yellow dye and Kahwa tea carbon system.

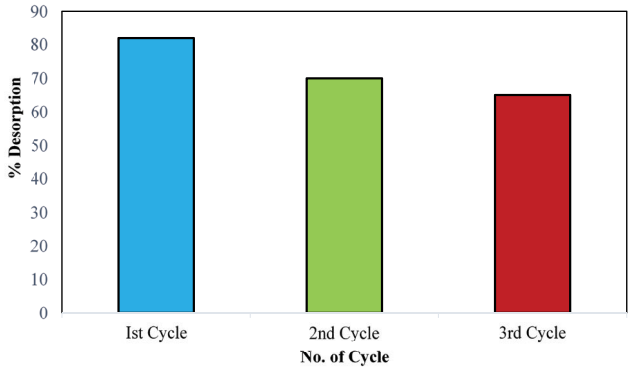

Fig. 13. Desorption of dye and regeneration of adsorbent.

Acknowledgments

Authors (JM and AM) are grateful to the Ministry of Human Resource Development of the Government of India for financial support through the SPARC initiative (project: SPARC/2018-2019/P307/SL).

References

[1] K. Hunger, P. Mischke, W. Rieper, R. Raue, K. Kunde, A. Engel, Azo Dyes, C. Ley, Ullmann's Encyclopedia of Industrial Chemistry, Wiley-VCH, Weinheim, Germany, 2000.
[2] A. Bafana, S.S. Devi, T. Chakrabarti, Azo dyes: past, present and the future, Environ. Rev., 19 (2011) 350–371.

[3] M.A. Brown, S.C. De Vito, Predicting azo dye toxicity, Crit. Rev. Env. Sci. Technol., 23 (1993) 249–324.
[4] K. Golka, S. Kopps, Z.W. Myslak, Carcinogenicity of azo colorants: influence of solubility and bioavailability, Toxicol. Lett., 151 (2004) 203–210.
[5] J. Mittal, Synthetic food dyes permitted in India, Resonance – J. Sci. Educ., 25 (2020) 567–577.
[6] T. Robinson, G. McMullan, R. Marchant, P. Nigam, Remediation of dyes in textile effluent: a critical review on current treatment technologies with a proposed alternative, Bioresour. Technol., 77 (2001) 247–255.
[7] C. Allegre, M. Maisseu, F. Charbit, P. Moulin, Coagulation–flocculation–decantation of dye house effluents: concentrated effluents, J. Hazard. Mater., 116 (2004) 57–64.
[8] A.H. Essadki, M. Bennajah, B. Gourich, Ch. Vial, M. Azzi, H. Delmas, Electrocoagulation/electroflotation in an external-loop airlift reactor—application to the decolorization of textile dye wastewater: a case study, Chem. Eng. Process., 47 (2008) 1211–1223.
[9] R. Jain, M. Mathur, S. Sikarwar, A. Mittal, Removal of the hazardous dye Rhodamine B through photocatalytic and adsorption treatments, J. Environ. Manage., 85 (2007) 956–964.
[10] W.G. Kuo, Decolorizing dye wastewater with Fenton's reagent, Water Res., 26 (2004) 881–886.
[11] I. Anastopoulos, I. Pashalidis, A.G. Orfanos, I.D. Manariotis, T. Tatarchuk, L. Sellaoui, A. Bonilla-Petriciolet, A. Mittal, A. Núñez-Delgado, Removal of caffeine, nicotine and amoxicillin from (waste)waters by various adsorbents. A review, J. Environ. Manage., 261 (2020) 110236, doi: 10.1016/j.jenvman.2020.110236.
[12] I. Anastopoulos, A. Mittal, M. Usman, J. Mittal, G.H. Yu, A. Núñez-Delgado, M. Kornaros, A review on halloysite-based adsorbents to remove pollutants in water and wastewater, J. Mol. Liq., 269 (2018) 855–868.
[13] J. Mittal, A. Mittal, Chapter 11 – Hen Feather: A Remarkable Adsorbent for Dye Removal, S.K. Sharma, Ed., Green Chemistry for Dyes Removal from Wastewater: Research Trends and Applications, Scrivener Publishing LLC, USA, 2015, pp. 409–457.
[14] A. Mittal, M. Teotia, R.K. Soni, J. Mittal, Applications of egg shell and egg shell membrane as adsorbents: a review, J. Mol. Liq., 223 (2016) 376–387.
[15] A. Mittal, R. Ahmad, I. Hasan, Biosorption of Pb^{2+}, Ni^{2+} and Cu^{2+} ions from aqueous solutions by L-cystein-modified montmorillonite-immobilized alginate nanocomposite, Desal. Water Treat., 57 (2016) 17790–17807.
[16] A. Mittal, R. Ahmad, I. Hasan, Iron oxide-impregnated dextrin nanocomposite: synthesis and its application for the biosorption of Cr(VI) ions from aqueous solution, Desal. Water Treat., 57 (2016) 15133–15145.
[17] K.Z. Elwakeel, A.A. El-Bindary, A.Z. El-Sonbati, A.R. Hawas, Magnetic alginate beads with high basic dye removal potential and excellent regeneration ability, Can. J. Chem., 95 (2017) 807–815.
[18] N. Hassan, A. Shahat, A. El-Didamony, M.G. El-Desouky, A.A. El-Bindary, Synthesis and characterization of ZnO nanoparticles via zeolitic imidazolate framework-8 and its application for removal of dyes, J. Mol. Struct., 1210 (2020) 128029, doi: 10.1016/j.molstruc.2020.128029.
[19] S. Dubey, S. Banerjee, S.N. Upadhyay, Y.C. Sharma, Application of common nano-materials for removal of selected metallic species from water and wastewaters: a critical review, J. Mol. Liq., 240 (2017) 656–677.
[20] V.K. Gupta, Application of low-cost adsorbents for dye removal – a review, J. Environ. Manage., 90 (2009) 2313–2342.
[21] K.S. Bharathi, S.T. Ramesh, Removal of dyes using agricultural waste as low-cost adsorbents: a review, Appl. Water Sci., 3 (2013) 773–790.
[22] M. Sulyman, J. Namiesnik, A. Gierak, Low-cost adsorbents derived from agricultural by-products/wastes for enhancing contaminant uptakes from wastewater: a review, Pol. J. Environ. Stud., 26 (2017) 479–510.
[23] Titan Yellow, $C_{28}H_{19}N_5Na_2O_6S_4$, PubChem (nih.gov).
[24] K. Zare, H. Sadegh, R. Shahryari-ghoshekandi, B. Maazinejad, V. Ali, I. Tyagi, S. Agarwal, V.K. Gupta, Enhanced removal of toxic Congo red dye using multi walled carbon nanotubes: kinetic, equilibrium studies and its comparison with other adsorbents, J. Mol. Liq., 212 (2015) 266–271.
[25] M. Rastgordani, J. Zolgharnein, V. Mahdavi, Derivative spectrophotometry and multivariate optimization for simultaneous removal of Titan yellow and Bromophenol blue dyes using polyaniline@SiO_2 nanocomposite, Microchem. J., 155 (2020) 104717, doi: 10.1016/j.microc.2020.104717.
[26] M. Monier, D.A. Abdel-Latif, H.A. Mohammed, Synthesis and characterization of uranyl ion-imprinted microspheres based on amidoximated modified alginate, Int. J. Biol. Macromol., 75 (2015) 354–363.
[27] L. Shi, S. Gunasekaran, Preparation of pectin–ZnO nanocomposite, Nanoscale Res. Lett., 3 (2008) 491–495.
[28] S. Hiremath, M.A.L. Antony Raj, M.N. Chandra Prabha, C. Vidya, *Tamarindus indica* mediated biosynthesis of nano TiO_2 and its application in photocatalytic degradation of Titan yellow, J. Environ. Chem. Eng., 6 (2018) 7338–7346.
[29] X.T. Cheng, N. Li, M.F. Zhu, L.L. Zhang, Y. Deng, C. Deng, Positively charged microporous ceramic membrane for the removal of Titan yellow through electrostatic adsorption, J. Environ. Sci., 44 (2016) 204–212.
[30] R. Ahmad, A. Mirza, Adsorptive removal of heavy metals and anionic dye from aqueous solution using novel xanthan gum-glutathione/zeolite bionanocomposite, Groundwater Sustainable Dev., 7 (2018) 305–312.
[31] C.L. Jiang, X.H. Wang, D.M. Qin, W.X. Da, B.X. Hou, C. Hao, J.B. Wu, Construction of magnetic lignin-based adsorbent and its adsorption properties for dyes, J. Hazard. Mater., 369 (2019) 50–61.
[32] R. Ahmad, A. Mirza, Synthesis of guar gum/bentonite a novel bionanocomposite: isotherms, kinetics and thermodynamic studies for the removal of Pb(II) and crystal violet dye, J. Mol. Liq., 249 (2018) 805–814.
[33] V.K. Gupta, S. Agarwal, R. Ahmad, A. Mirza, J. Mittal, Sequestration of toxic congo red dye from aqueous solution using ecofriendly guar gum/activated carbon nanocomposite, Int. J. Biol. Macromol., 158 (2020) 1310–1318.
[34] S. Soni, P.K. Bajpai, J. Mittal, C. Arora, Utilization of cobalt doped Iron based MOF for enhanced removal and recovery of methylene blue dye from waste water, J. Mol. Liq., 314 (2020) 113642, doi: 10.1016/j.molliq.2020.113642.
[35] V.K. Gupta, A. Mittal, L. Krishnan, J. Mittal, Adsorption treatment and recovery of the hazardous dye, brilliant blue FCF, over bottom ash and de-oiled soya, J. Colloid Interface Sci., 293 (2009) 16–26.
[36] V.K. Gupta, A. Mittal, V. Gajbe, J. Mittal, Adsorption of basic fuchsin using waste materials, bottom ash and de-oiled soya as adsorbent, J. Colloid Interface Sci., 319 (2008) 30–39.